

Comparison of digital aerial image and LiDAR data to estimate forest parameters

Shrota Shrestha
May, 2013

Comparison of digital aerial image and LiDAR data to estimate forest parameters

by

Shrota Shrestha

Thesis submitted to the Faculty of Geo-Information Science and Earth observation (University of Twente) in partial fulfilment of the requirements for the degree of Master of Science in Geo-information Science and Earth Observation, Specialisation: (Geo-Information Science and Earth Observation for Environmental Modelling and Management)

Supervisors

Dr. Y.A.Hussin

Dr. M.J.C. Weir

Thesis Assessment Board

Name Examiner (Prof. Dr. A.K.Skidmore)

Name Examiner (Dr. ir. S.J. Oude Elberink)



UNIVERSITY OF TWENTE.

ITC

FACULTY OF GEO-INFORMATION SCIENCE AND EARTH OBSERVATION

Course Title: Geo-Information Science and Earth Observation for Environmental Modeling and Management

Level: Master of Science (MSc)

Course Duration: August 2011 – June 2013

Consortium Partners: Lund University (Sweden)
University of Twente, Faculty ITC (The Netherlands)
University of Southampton (UK)
University of Warsaw (Poland)
University of Iceland (Iceland)
University of Sydney (Australia)

Disclaimer

This document describes work undertaken as part of a programme of study at the Faculty of Geo-Information Science and Earth observation (University of Twente). All views and opinions expressed therein remain the sole responsibility of the author, and do not necessarily represent those of the institute.

Abstract

The estimation of forest parameters plays important role on forest inventory. The forest inventory is expensive and time consuming, but also important on forest management. The development on remote sensing techniques such as digital aerial images, satellite images, LiDAR has provide more efficient way of forest inventory. Many researches are going on to study more accurate and efficient way of forest inventory using different remote sensing techniques. This study aims to demonstrate the accuracy of estimation of forest parameters by using digital aerial image and LiDAR. In addition with, the potential LiDAR metrics were selected to estimate height, basal area and volume.

The plot based approach was adopted as the study area has 1.0 point density m^{-2} and was not enough to generate the height, basal area and volume on individual tree level. Eight LiDAR metrics were selected for basal area model and seven LiDAR metrics were selected for height model and validated with field measured data. The final model was determined with selected LiDAR metrics after stepwise selection procedures. 10th and 90th percentiles of LiDAR canopy height was selected for final height model and maximum and mean of LiDAR canopy heights, 50th, 75th and 90th percentiles of LiDAR canopy heights, coefficient of variation of LiDAR canopy heights and canopy cover density was selected for final basal area model. While volume model used LiDAR tree height estimated after stepwise selection procedures and canopy density metrics from LiDAR data. The coefficient determination for height, basal area and volume was found to be 71%, 78% and 81% respectively with field measured data.

Due to low GSD and low forward overlap on aerial image generate poor quality DSM and DTM, which affect the quality of CHM. The height of tree cannot be extracted from aerial image CHM and further analysis cannot be performed on this study area with aerial image CHM.

Acknowledgements

I am highly indebted to Dr. Yousif Hussin who contributed as my first supervisor and provides guidance, valuable suggestions, constructive comments and encouragements throughout the undertaking of the research and writing works. I am deeply honoured and would like to express my sincere gratitude to my supervisor Dr. Michael Weir for his continuous support, valuable suggestions and assistance during my whole research

I would like to extend my profound appreciation to Dr. Kourosh Khoshelham for his valuable support, guidance, co-operation and facilitating my research. I would like to express my deep gratitude to Mr. Thomas Brethvad for providing the valuable advice and a suggestion has been a great help in formulating the research in a scientific way.

I also sincerely owe to Mr. Bob McGaughey who provided technical guidance, valuable suggestions on Fusion/LDV software.

I wish to acknowledge the assistance provided by Mr. Grigorijs Goldbergs was greatly appreciated

I am also grateful to and COWI, Norway team for their kind support in providing me immensely valuable data and information relating to the research.

I would also like to express my great appreciation to my GEM classmates Lina, Joana, Collins and Joaquin for their valuable suggestions, moral support and technical assistance throughout the research. Sincerely thanks to each one of you. Special thanks go to, Sunil Thapa, Arun Poudyal, Sujata Gautam and Reshma Shrestha for their valuable guidance, suggestions and remarks. My sincere thanks go to Chandra Prasad Ghimire for his guidance on statistical analysis of the research.

Last but not the least, deepest appreciation to my respected parents, brother and sister who always gave me the strengths and been a source of inspiration to every piece of my work.

Shrota Shrestha
2013

Table of Contents

Abstract	v
Acknowledgements.....	vi
List of figures	ix
List of tables	x
1. Introduction	1
Background 1	
1.1 Aerial Photogrammetry	2
1.2 Image Matching	4
1.3 Principal of LiDAR	5
1.4 Point cloud based on aerial image and LiDAR	6
1.5 Problem statement and Justification	7
1.6 Research Objectives	8
1.7 Research Question	9
1.8 Research Hypothesis	9
2. Study area and Data	10
2.1 Study area	10
2.2 Description of data.....	11
2.2.1 LiDAR data	11
2.2.2 Aerial Imagery data	11
2.2.3 Field data	12
3. Method.....	14
3.1 LiDAR data processing	15
3.1.1 Digital Elevation Model extraction	15
3.1.2 Extraction of field plots.....	17
3.1.3 Extraction of LiDAR metrics	18
3.2 Aerial Image data processing.....	18
3.2.1 Data Import to SOCET GXP	18
3.2.2 Aerial Triangulation.....	19
3.2.3 Automatic Terrain Generation (ATG)	20
3.2.4 Extraction of CHM from DSM and DTM.....	21
3.3 Regression Analysis	22
3.3.1 Estimating dominant tree height and basal area from LiDAR data	22
3.3.2 Estimating stand volume from LiDAR data.....	22
4. Results	23
4.1 Descriptive analysis of field data	23
4.2 DSM, DTM and CHM generation from LiDAR data	24
4.3 Extraction of field plots from LiDAR data	25
4.4 Accuracy assessment	25
4.4.1 LiDAR derived height.....	25
4.4.2 Basal Area.....	27
4.5 Correlation analysis.....	28
4.6 Stepwise Regression	29

4.7	Model validation of tree height and basal area	29
4.8	Model for stand volume	30
4.9	DSM, DTM and CHM generation from aerial 3D image	32
5.	Discussion	34
5.1	Extraction of LiDAR metrics	34
5.2	LiDAR derived tree height and basal area and accuracy assessment	34
5.3	Model validation of tree height and basal area	36
5.4	LiDAR derived stand volume and accuracy assessment	36
5.5	Aerial image analysis.....	37
6	Conclusion and Recommendations	39
6.1	Conclusions	39
6.2	Recommendations	39
	References.....	40

List of figures

Figure 1-1: Computer vision algorithms generate 3D "point clouds" by building geometry from matching features identified in multiple overlapping photographs. 3D point clouds are then geo-referenced and used to make measurement	5
Figure 1-2: Typical operation of LiDAR Scanning	6
Figure 2-1: Study area with field plots and aerial image with stand plots	10
Fig 2-1: shows camera calibration data	12
Figure 3-1: Flowchart of research method	14
Figure 3-2: LiDAR points over the single tree and closed canopy tree	15
Figure 3-3: DSM (green) over the DTM (grey)	16
Figure 3-4: Shows the workspace manager and frame import tools in SOCET GXP	19
Figure 3-5: Triangulation window with ground point file and APM tab	20
Figure 3-6: Automatic terrain generation tab	21
Figure 4-1: Lorey's mean height (PR= Pinus sylvestris, PA= Picea abies, BP= Betula pubescens)	23
Figure 4-2: basal area PR= Pinus sylvestris, PA= Picea abies, BP= Betula pubescens)	23
Figure 4-3: volume of major tree species	24
Figure 4-4: (a) DTM and (b) CHM derived from LiDAR point cloud using Fusion software	24
Figure 4-5: Cross-section (a) and overhead view (b) for the same field plot	25
Figure 4-6: Scatterplot and summary of regression for tree height measurements	26
Figure 4-7: Scatterplot and summary of regression for basal area measurements	27
Figure 4-8: Scatterplot of observed and predicted height and basal area	30
Figure 4-9: Scatterplot of observed and predicted stand volume	31
Figure 4-10: shows the (a) DTM and (b) DSM from aerial image	32
Figure 4-11: shows the (a) CHM and (b) aerial image of the same area	32
Fig 5- 1 Comparison of CHM derived from aerial image, LiDAR and aerial photographs of the same area from up to bottom respectively	38

List of tables

Table 2-1: Metadata of the LiDAR data.....	11
Table 4-1: Descriptive statistics of field plots	23
Table 4-2: Summary of statistics for tree height measurement	26
Table 4-3: Summary of ANOVA analysis for tree height.....	26
Table 4-4: Summary of statistics for basal area measurement	27
Table 4-5: Summary of ANOVA test for basal area measurement....	28
Table 4-6: Correlation among the variables of regression model	28
Table 4-7: Regression coefficients and statistics of model.....	31
Table 4-8: Summary of ANOVA analysis for volume model	31

1. Introduction

Background

In forest management, forest inventory plays an important role as it provides the information that is required to make decisions(Kangas, Heikkinen et al. 2004). Forest inventory is basically performed to provide the accurate measurements and estimations of the current state of the forest for planning and management(Tomppo 2010). In forests that are exploited for timber production, accurate estimation of forest parameters especially the volume of growing stock, biomass, carbon content and the area of certain type of forest are the main information needed for sustainable management(Kangas, Heikkinen et al. 2004). According to the user's requirement, forest inventory can be done by applying different methods using either field surveys or remote sensing or a combination of both(Packalen 2009). Remote sensing data such as satellite images, digital aerial photographs and LiDAR (Light Detection and Ranging) are mostly used in forest inventories and have potential for forest parameters estimation(Junttila 2011),(Magnusson 2006). The rapid development on remote sensing has become an integral part of forest inventory and management in reducing the forest expenses and collecting the data faster(Næsset 2002). The development of digital aerial photogrammetry and LiDAR has increased the possibility of new applications in forest inventory(Korpela 2004).

For accurate estimation of biomass, carbon, and other land management, information about the 3D vegetation structure in high spatial resolution is essential. The demand for these measurements has grown rapidly in aspect of modeling and management. In recent years, LiDAR has been preferred tool for these measurements and making measurements of the 3D vegetation structure. For decades, aerial photogrammetric tools have been used to interpret 3D surfaces from 2D stereo image pairs(Dandois and Ellis 2010). Aerial photographs have advantages on 3D measurements for accurate estimation of forest parameters; nevertheless they are often used only for 2D measurements(Korpela 2004). After the commercial development of Aerial Laser Scanning, photogrammetric measurement was expected to be taken over by LiDAR. But still the

most promising remote sensing technologies are LiDAR and digital aerial photographs for accurate and efficient forest inventory(Holopainen 2004). Similarly, the integration of LiDAR and digital aerial images has many advantages. Aerial photo images have geometric stability which provides references for laser point cloud. The integration also compensates the weakness on each method which provide more accurate on modeling, interpretation and classification of the objects (Baltsavias 1999).

1.1 Aerial Photogrammetry

Aerial photography has been the most used remote sensing data for decades in collecting the forest data for interpretation, forest mapping, estimation of stand attributes and tree composition(Korpela 2004),(Wulder 2003) . As early as the 1920s, many studies and experiments were performed in Europe and North America by using aerial photographs such as interpretation of stereo aerial photographs for estimation of forest information. Finnish forestry used it for preliminary studies in early 1920s and used it for forest mapping and estimation of growing stock from 1930s(Packalen 2009). Also, with the help of aerial photographs, many forest inventories have been carried out to delineate and estimate forest variables in Sweden and Norway(Magnusson, Fransson et al. 2007).

The paradigm shift in aerial photogrammetry from analog to analytical to computer assisted and to digital photogrammetry has encourage the foresters to research on forestry (Balenovic 2012), (Madani 2001),(Leberl 2010). Aerial images started to be digitized in 70's and 80's, but commercial airborne digital imaging sensors were not launched until 2000(Cramer 2005). The acceptance of digital camera is due to economy and the advantage of innovative data products (large format imaging sensors) which became powerful alternative to the analogue imaging(Cramer 2005). Digital aerial cameras can take many images the users need and the cost will not increase, in fact it will decrease (Leberl 2010).

Aerial photographs can be used in both ways manual and automatic interpretation. By manual interpretation of aerial images using stereoscopic view can be used on stand delineation, tree height measurements and tree species composition(Magnusson, Fransson et

al. 2007). The accuracy of photo interpretation depends on the nature of objects, quality of images and interpretation procedure(Lillesand T. M. & Kiefer R. W. 2000). However, manual interpretation is time consuming, labor intensive and expensive also(Ke 2009), (Wang, 2004). Digital photogrammetry can be used with digital images and scanned analog photographs(Madani 2001). Stereo photography lacks spectral depth and satellite image have more spectral bands but not of high resolution and geometric precision(Tuominen and Pekkarinen 2005),(Gong, Biging et al. 1999).

The functions of digital Photogrammetry can be divided into categories: i. Film scanning, ii. Aerial triangulation, iii. Digital terrain elevation, iv. Orthophoto generation, v. 3D data(Leberl 2010). Digital photogrammetry encompasses both high spatial and spectral resolution with sufficient spectral bands(Gong, Biging et al. 1999). For digital aerial photogrammetry, very high resolution imageries are available which has spatial resolution (10cm to 2- 3m) and can estimate forest stand characteristic more accurately(Tuominen and Pekkarinen 2005). Digital image can be acquired from digital camera or scanning an analogue photograph. The quality of digital image depends upon the parameters of CCD (Charge-coupled device) chips, i.e. photosensitive parts of sensors, digital cameras and sensors. Easy data transfers or large spectral sensitivity are the major advantages of digital image(Potuckova 2004). Digital photogrammetry is computerized application which automates all the traditional photogrammetry procedure such as contour and orthophoto generation, stereo model construction, aerial triangulation, photo orientation, mosaicking and mapping. The development of spatial positioning technology, remote sensing technology, and computer developed the aerial triangulation which progressed on digital mapping without GCPs(Yuan 2008). The primary use of digital photogrammetry is to produce digital elevation models and orthophoto(Gong, Biging et al. 1999). The digital aerial photographs can be interpreted as 2D and 3D image. 2D image include information such as species and number of trees but not auxiliary information such as tree locations, crown closure and crown size. For forest parameter estimation, 3D based interpretation is preferred. 3D automatic interpretation develops with digital photogrammetry can produce many forest parameters such as tree location, height, crown depth, crown radius and crown surface curvature(Gong 2002).

Spatial, tonal and textural properties of aerial image determine the interpretation of forest attributes(Wulder 2003). The scanned digital orthophoto has been used widely in forest sector for estimation of area, distance, tree height (Olsson 2005),(Zagalikis, Cameron et al. 2005) The recent development in algorithms to generate 3D data from automatic matching of aerial imagery has created a revolution on estimating forest parameters (Bohlin, Wallerman et al. 2012)

1.2 Image Matching

Digital surface models (DSM) can be generated from different sources such as LiDAR, aerial images, satellite images and RADAR for analysis of vegetation, erosion(Sohraib 2012). DSM can be achieved from automatic image matching(Waser, Baltsavias et al. 2008). Image Matching is increasing the demand of accurate and low price for extraction of DSM. The quality of images, orientation and camera calibration will determine the quality of DSM. The high forward/side overlap such as 80/60 or 90/70 (both percent) significantly reduces occlusion in forest areas and has probability of higher accuracies and reliability (Lemaire 2008; Waser, Baltsavias et al. 2008). The area-based image matching and feature-based image matching has to be considered to create more redundant matches and for appropriate matching(Zhang 2006). The geometry accuracy of DSM from image matching depends upon the correction of image coordinated from bundle block adjustment(Haala 2009). Image matching is increasing interest on the field of photogrammetric society to create accurate and dense point cloud for digital elevation model (DEM) which can be an alternative technique to LiDAR(Gulch 2009). Lothammer (2008) suggested that for derivation of DSM, resolution should be at least 20 cm Ground sampling distance (GSD), calibrated digital camera and at least 60/60 overlap which give DSM five times of image GSD and height accuracy approximately two times of image GSD. The photogrammetric matching of aerial image can estimate tree height, stem volume and basal area comparable to LiDAR(Bohlin, Wallerman et al. 2012). More accurate tree height estimates can be obtained from digital photogrammetric by improved image matching (Næsset 2002)Point clouds provide accurate analysis of automatic image based 3D data collection(Cramer 2009).

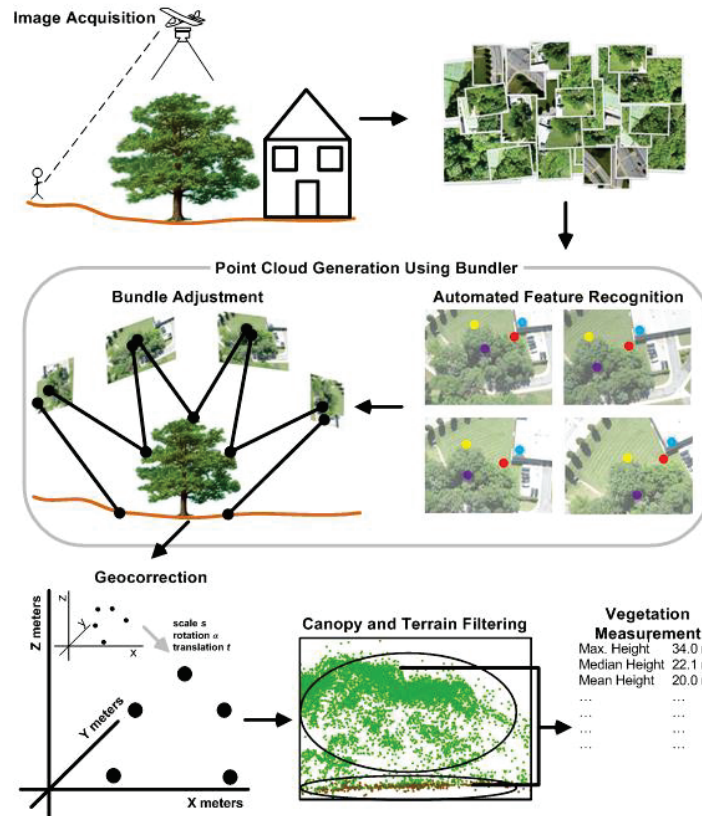


Figure 1-1: Computer vision algorithms generate 3D "point clouds" by building geometry from matching features identified in multiple overlapping photographs. 3D point clouds are then geo-referenced and used to make measurement

(Dandois and Ellis 2010)

1.3 Principal of LiDAR

LiDAR is the active optical remote sensing technology which emits highly directional laser pulses and mainly used for small area inventories (Junntila 2011). With the help of global positioning system (GPS), inertial measurement unit (IMU), position and altitude of laser scanner, LiDAR determine the position (X, Y, Z) of the objects. The laser scanner emits near infra-red laser pulses at high frequency of 25,000 to 100,000 per second. Most LiDAR system has capability to detect 2-5 reflected returns per laser pulse. For terrain mapping, LiDAR is flown over the leaf-off conditions while for vegetation

mapping; it is flown over leaf-on conditions (McGaughey 2006). LiDAR is mostly used to accurately estimate the topography of the area and obtain vertical information of the object. The major mapping applications of LiDAR data are vegetation mapping and topographic mapping.

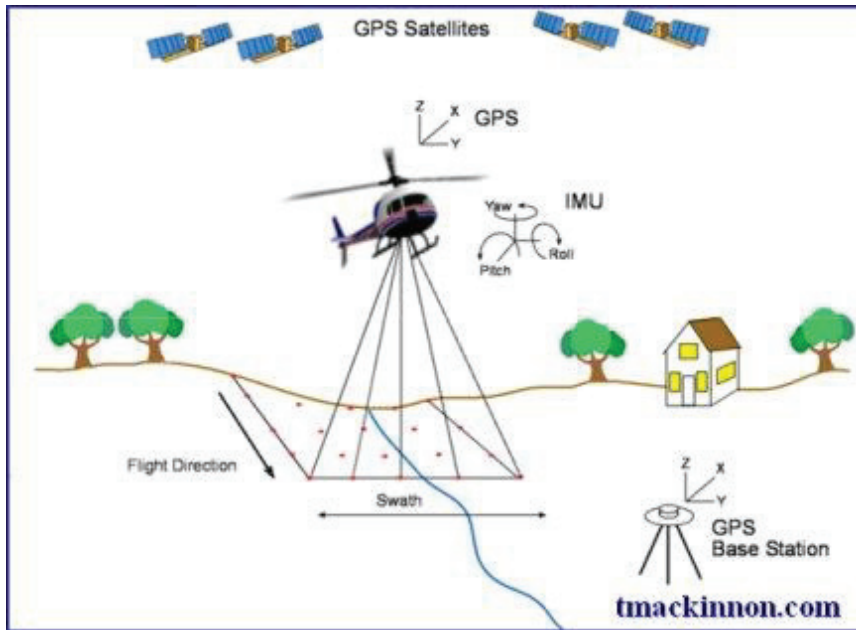


Figure 1-2: Typical operation of LiDAR Scanning

(Source: www.tmackinnon.com)

Small foot prints (less than 1 m) use discrete points (X, Y, Z and intensity) for DTM extraction and forest inventory (Kukko 2009).

1.4 Point cloud based on aerial image and LiDAR

Photogrammetry has the long history of developments on automation of information extraction from digital images while LiDAR is the important technologies developed recently (Baltsavias 1999). LiDAR data are referred to as better accuracy for last decade but the advent of new digital aerial cameras with wide coverage sensors, excellent signal to noise ratio and high forward overlap capability is more suitable and efficient for image matching and to create point cloud. Despite the fact that tools for automatic stereo image matching have

been available for more than two decades, the collection of high resolution, high accuracy elevation data was mainly dominated by the application of airborne LiDAR systems(Haala 2009).

The concept of point cloud generation from image matching is still new and in a development phase. However, there are studies that suggest the point cloud from image matching can be alternative technique to LiDAR for DSM preparation. Lemaire (2008) reported that DSM can be generated from image matching using MATCH-T software which is competitive to LiDAR especially if produced from high resolution (<20cm) orthophoto. The DSM point cloud from image matching is more accurate on flat terrain rather than on sloping surfaces. Waser,et.al.(2008) generated DSM from aerial image of spatial resolution 0.5m and co-registration was done with DSM from LiDAR (1-2 points m²). On the other study, DEM for open pit mining area were generated automatically from MATCH-T software which was accurate enough to compare with manual measurements(Gulch 2009). Leberl (2010) came up with "Point clouds: LiDAR versus 3D vision" which illustrate on the benefits of point clouds based upon aerial image and they came with 15 advantages of photogrammetric approach to LiDAR. Point clouds from digital photogrammetry are superior to LiDAR point cloud and have accuracy of more than ± 1 pixel whereas LiDAR accuracy is based on GPS/IMU measurements. Bohlin, Wallerman et al. (2012) estimated the tree height, stem volume and basal area with high accuracy using image matching of digital aerial image in combination with high resolution image. For tree height, stem volume, basal area the result shows RMSEs of 8.8%, 13.1% and 14.9% respectively at stand level. (Kamiya 2012) also describe the collection of forest resource management 3D data acquired from stereo matching of aerial photographs (20cm GSD). DSM and DTM generated from aerial images provide enough accuracy to manage forest resources.

1.5 Problem statement and Justification

Various methods for the derivation of forest parameters in the fields of pre-processing, DSM generation, tree extraction, and classification already exist, but few of them are targeted or even tested on most recent point cloud based on digital aerial image.

1. The operational cost for LiDAR is high.
2. LiDAR has poor capability on textural and spectral information which can be substitute by digital aerial images.
3. LiDAR can penetrate to the ground in dense forest that does not mean the pulse will always hit the ground which can give wrong information.
4. LiDAR can only map in 3D while photogrammetry can produces both in 2D and 3D maps(Leberl 2010).
5. LiDAR is applicable to estimate tree height with high accuracy but not to estimate tree species and tree density(Kamiya 2012).
6. Aerial photogrammetric can produce more point density than LiDAR at the same height and flight speed which is more useful for interpretation. 60% side lap between flight line will also reduce occlusion. The comparison table below provides the further justification.

Table 1-1: Comparison between LiDAR and Digital Photogrammetry(Leberl 2010)

LiDAR	Digital photogrammetry
170 scans per second(190 kHz)	GSD 25 cm
8 points/m ²	16 points/m ²
flying height 750 meters	flying height 4188 meters
aircraft speed 60m/sec	aircraft speed 141m/sec
	60% side lap between flight line
20% side lap between flight line	line
efficiency 17%	efficiency 100%

1.6 Research Objectives

The main objective of the research is to compare method to accurately estimate forest parameters of Bergvik Skog AB, Sweden.

Specific objectives

- a. To select the potential LiDAR metrics to generate tree height, basal area and volume.
- b. To compare the accuracies of tree height, basal area and volume derived from aerial image 3D and LiDAR point cloud.

1.7 Research Question

- a. Which LiDAR metrics estimate more accurate tree height, basal area and volume compare to field measured tree height, basal area and volume?
- b. Which approaches (aerial image and LiDAR) gives the better accuracy on estimating forest parameters?

1.8 Research Hypothesis

- a. There is statistically significant difference in estimation of forest parameters (tree height, basal area and volume) using LiDAR, aerial image.
- b. The mean height from the digital aerial image is significantly more accurate than mean height from LiDAR point cloud.

2. Study area and Data

2.1 Study area

Sweden is regarded as an important forest nation in Europe. Sweden extends from southern Baltic sea to north of Arctic Circle. Although Sweden is situated in Northern Europe, the climate is fairly mild and temperate. Sweden has 29 million hectares of forest land (60% of the total land) among which 22.5 million hectares of forest is production forest. About 2.9 billion cubic meters of total standing volume is on productive forest land, which has been increased by 80% since 1920s. 50 % of Swedish forest area is owned by individual owners, 25% from privately owned companies, 14% from forest are state owned companies and rest 11% from other private, state and public owned companies (Swedish statistical yearbooks of forestry, 2012). The study area as shown in fig 2.1 is situated on Ockelbo

municipality, the central part of Sweden. It is located in the Gavleborg County (the latitude range from 60° N to 62° N) and has altitudinal range of 70-600 m above sea level.

Sweden is categorized in eight different vegetation zones under which Gavleborg County lies in south boreal vegetational zones. The area consists of 80% of Scots pine (*Pinus sylvestris*) and Norway spruce (*Picea abies*), while 20% of Birch (*Betula pubescens*) and Lodgepole pine (*Pinus contorta*) on the forest.

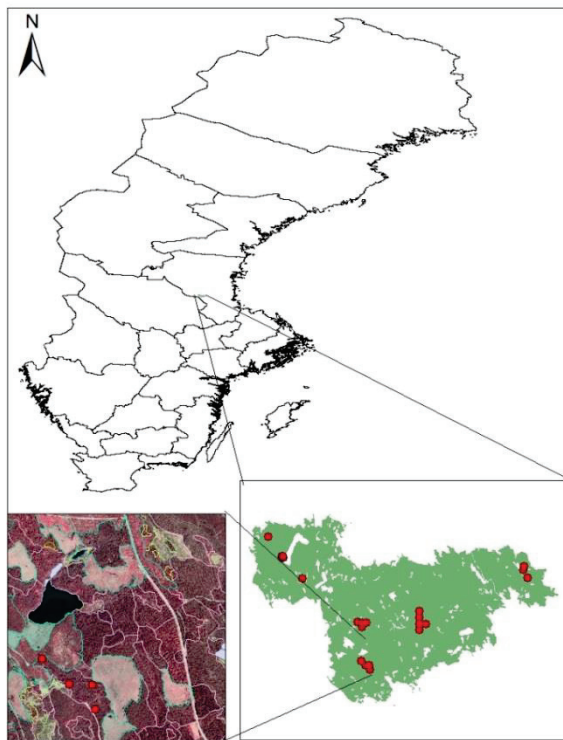


Figure 2-1: Study area with field plots and aerial image with stand plots

2.2 Description of data

The materials that have been used for this research are low density LiDAR data, aerial images, and field data. The digital aerial images and LiDAR data were collected from Lantmateriet, Sweden (<http://www.lantmateriet.se>) Field data were collected from Bergvik Skog, Sweden.

2.2.1 LiDAR data

The LiDAR data were collected in 2010 using scanner Optech ALTM Gemini/80. The scanning area size is 25*50 square kilometers that has at least 200 meters overlap on the adjacent sides. The scanning was mainly done in early spring and late autumn. The accuracy is of scanning is about 10 cm on planar paved surfaces but the accuracy decreases with the steep slope and dense forest. The measured accuracy in the height is about 30 cm. The number of points per file range from 3 million to 5 million The laser data were in the form of point clouds where each point has been classified to land, water or unclassified. The laser data were in 2.5 *2.5 km with 10 m resolution.

Table 2-1: Metadata of the LiDAR data

Colour	Point density	Point density	0.5 to 1.0 per square
Blue	> 0.5 pt/m ²	Flight altitude	1700-2300 m
Green	0.25- 0.5 pt/m ²	Scanning angle	±20 °
Yellow	0.0625-0.25 pt/m ²	Footprints	0.5 meters (small)
Red	<0.0625 pt/m ²	Height system	RH 2000
Black	0 pt/m ²		

2.2.2 Aerial Imagery data

Aerial images were captured at an altitude of 4800m, on different dates of August and September, 2011. The images have pixel resolution of 0.5m (GSD) with radiometric resolution of 8 bits. Each image tile covers an area of 6.6 X 3.7 km square on the ground. Total

16 aerial images on 2 strips were used for the study area. The images had 60% forward overlap and 20-30% side overlap

The aerial images were in .TIFF file format and were taken by digital mapping camera (DMC). The sensor size of camera had width of 7680 pixels and length 13824 pixels with focal length of 120 mm. Aerial images were used to generate DSM and DEM using SOCET- GXP software. (Source: Lantmateriet photogrammetry, Sweden).

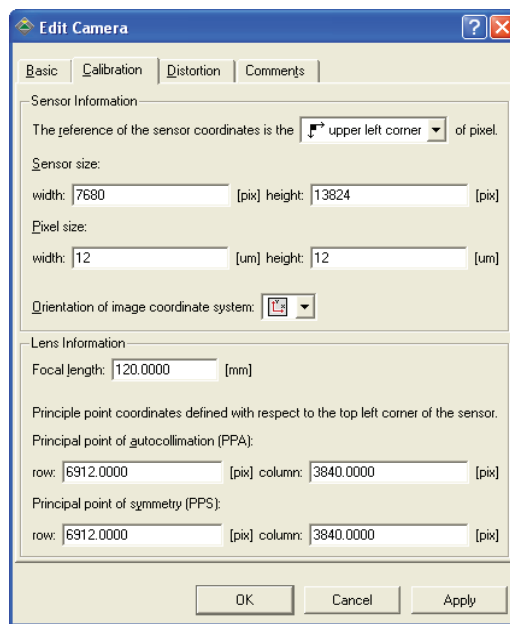


Fig 2-1: shows camera calibration data

2.2.3 Field data

24 field plots of Ockelbo area were selected as a study area. The field plots were measured on January, 2012. For each plots, all the trees were measured within the radius of 8.46 m. Trees with diameter at breast height (DBH) above 4 cm are measured and 3 trees were systematically selected for measuring height and age. The heights of trees range were from 10- 25 meters. The Lorey's height for each plot was also computed which give the average tree height with average basal area. As larger trees were given more weight than smaller trees, the Lorey's height is larger than average height of trees. It is predicted that the canopy height estimated from LiDAR

data will be closer to this Lorey's height (Magnussen and Boudewyn 1998). The plot volume, stem number, basal area were averaged per hectare while mean height, mean diameter were weighted by basal area of each tree in the plot. Soil sites were classified either by site index class or site productivity class. Soil site index class was based on dominant height at a certain age (H_{100}) and was determined according to dominant height curve. Swedish site classes were based on productivity ($m^3/ha/yr$). Basal area weighted mean diameter was calculated by multiplying tree diameter at breast height (DBH) by its basal area and then dividing by sum of total stand basal area. Stem number per hectare provided the information on the amount of pre commercial thinning that had to be done.

3. Method

The method for this research is mainly focused in two parts, LiDAR data processing and Digital aerial image processing. The method of this research comprises of 3 parts: LiDAR data processing, Digital aerial image processing and model development. The LiDAR data and Digital aerial images were further processed to obtain DSM, DTM and CHM. LiDAR data was processed on Fusion/LDV software to generate LiDAR metrics whereas Digital aerial image was processed on SOCET GXP software to generate DSM and DTM. The LiDAR metrics generated from Fusion /LDV software were further analyzed to extract tree height, basal area and volume. The DSM and DTM generated from aerial image were further processed on Arc GIS to generate CHM. The tree height, basal area and volume thus obtained were validated with field measured tree parameters. A flow diagram showing the research methodology is illustrated on fig 3-1.

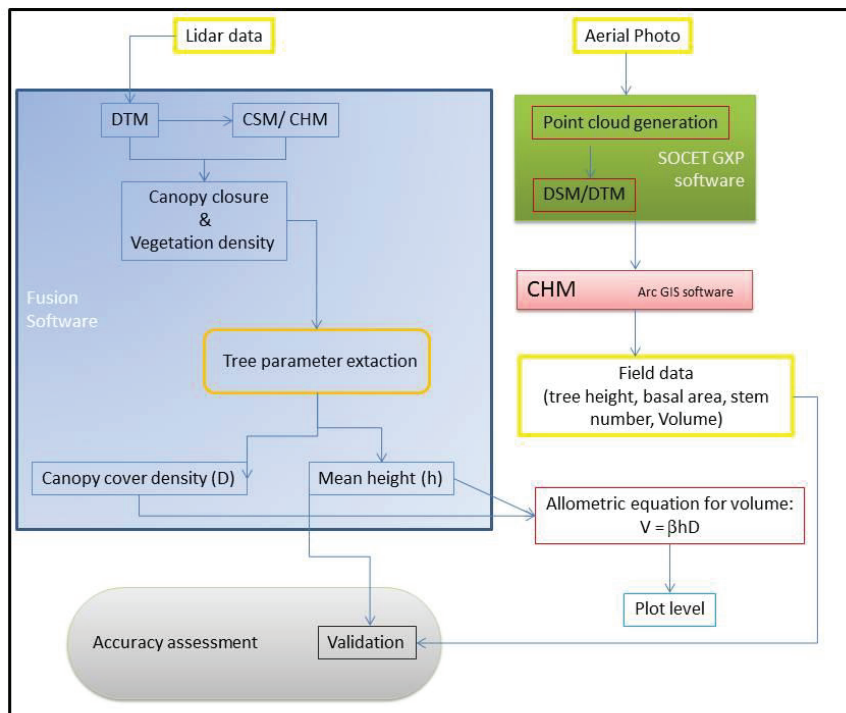


Figure 3-1: Flowchart of research method

3.1 LiDAR data processing

LiDAR point cloud was obtained from COWI. Terra scan software was used for pre-processing of raw LiDAR data by Lantmateriet (<http://www.lantmateriet.se>). The LiDAR point cloud was classified into 3 classes (ground, non-ground and unclassified) and has 5 returns. The LiDAR data were on LAS format.

DSM and DTM were generated from LiDAR data using Fusion/LDV Software. DSM is generated from first returns of the LiDAR point cloud.

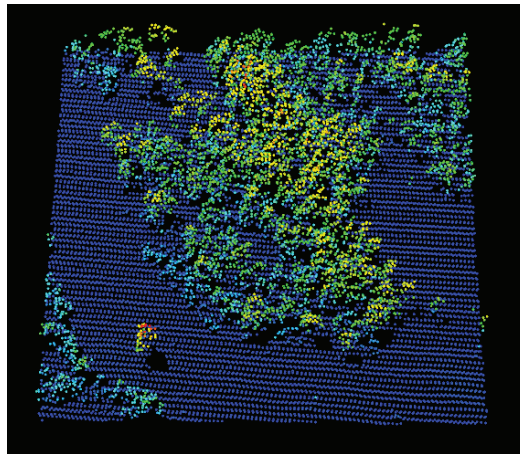


Figure 3-2: LiDAR points over the single tree and closed canopy tree

3.1.1 Digital Elevation Model extraction

Digital elevation model (DEM) represents the height information without any details about earth surface. DEM is often used as a general form of DSM and DTM.

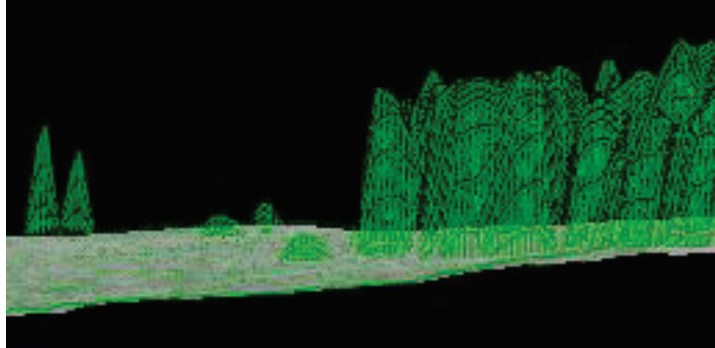


Figure 3-3: DSM (green) over the DTM (grey)

DTM provides the reference elevation of the features in the data which helps on measurement of heights. The above ground LiDAR returns were filtered and DTM was created with remaining ground LiDAR returns. DSM represents the earth's surface which includes all objects on it and useful to measure the height of the objects. The DSM is generated from first or highest return of the LiDAR point.

DTM

"Groundfilter" and "Gridsurfacecreate" command was execute in Window Dos command to create DTM from Fusion software. The syntax for DTM computation using GgridSurfacecreate command is:

```
GridSurfaceCreate out_path cellsize xyunits z units coordsys zone
horizdatum vertdatum in_path
```

DSM

"CanopyModel" command was execute to derive DSM. "CanopyModel" is for smoothing of the generated surface using median or mean filter or both which preserves local maxima to acquire tree tops. The syntax command for DSM computation is:

```
CanopyModel out_path cellsize xyunits z untis coordsys zone
horizdatum vertdatum in_path
```

CHM

CHM is also referred as normalised DSM as it is the difference between DTM and DSM to get the vegetation height. "CanopyModel" was executed to derive CHM. When used with DTM, CanopyModel subtracts the ground elevation from the DSM to produce CHM. The threshold height was defined to generate maximum tree height. The syntax for CHM is:

```
CanopyModel/ground: DTM_file out_path cellsize xyunits z units  
coordsys zone horizdatum vertdatum Lidar_data
```

Where,

Out_path = Output surface file

Cell size = Grid cell size for the surface

Xyunits = X and Y Units for LiDAR data

Z units = Elevation units for LiDAR data

Coordsys = Coordinate system for the surface

Zone = Coordinate system zone

Horizdatum = Horizontal datum for the surface

Vertdatum = Vertical datum for the surface

In_path = Input LiDAR file

3.1.2 Extraction of field plots

The sub-samples of LiDAR data were extracted in a fixed circular area for each plot. The Microsoft Excel was used to create the large batch files using plot centre coordinates and radius for each plot. The circumference for each plot was generated by calculating X and Y minimum and X and Y maximum by subtracting and adding radius to plot coordinates.

The LiDAR metrics were extracted for each plot by executing the "ClipData" command after the estimation of minimum X and Y and maximum X and Y for each plot. The syntax for extraction of field plots is:

```
ClipData /shape: 1 in_path out_path MInX MInY Max X MaxY
```

3.1.3 Extraction of LiDAR metrics

The descriptive statistics parameter for each LiDAR file and within each cell in the output grid is computed using "CloudMetrics" and "GridMetrics". The Metrics were created using point elevations and intensity values. The LiDAR metrics were used further for regression analysis. Cloudmetrics compute the single metrics for entire data file processed while Gridmetrics compute metrics for all returns within each cell.

```
Cloudmetrics /id/new/above:15 / minht: 2 in_path out_path
```

3.2 *Aerial Image data processing*

The SOCET set GXP software was used to process the digital aerial image. The different steps like data import, triangulation, and terrain generation were followed to generate DSM and DTM from aerial images.

3.2.1 Data Import to SOCET GXP

The data were imported, viewed, organized and performed on the workspace manager of the SOCET GXP. Before performing the task, the working directory was created where the desired spatial reference system was set for the project. Frame images, ground control points, camera calibration files and camera orientation data were imported on SOCET GXP.

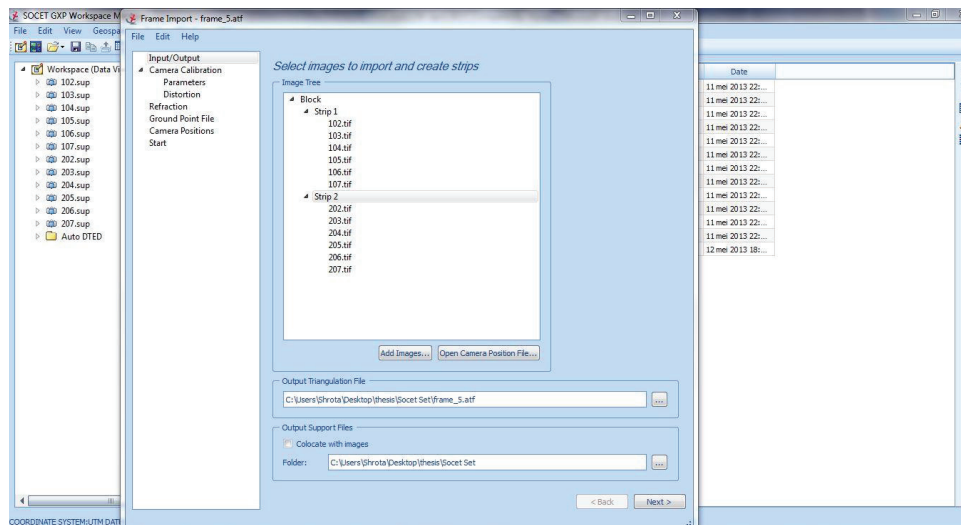


Figure 3-4: Shows the workspace manager and frame import tools in SOCET GXP

The frame import window consists of image files to import, camera calibration parameters, distortion, ground point file and camera position. After the frame import process is complete, a set of support files (.sup files) was created which provide geo referencing to aerial triangulation. Automatic DTED file was created by using camera calibration files and images.

3.2.2 Aerial Triangulation

Triangulation is the process of image orientation and registration to the ground. The triangulation tools on SOCET GXP have Image setup, Data setup, APM/IPM and solve tab. The images were import on image setup tab. Ground point files, automatic DTED (elevation) file were uploaded on the Data setup tab to increase the accuracy of the triangulation. APM (Automatic Point Measurement) helps to correlate the ground point on multiple images, producing tie points. Tie point pattern and strategies for automatic point measurement was selected on APM tab.

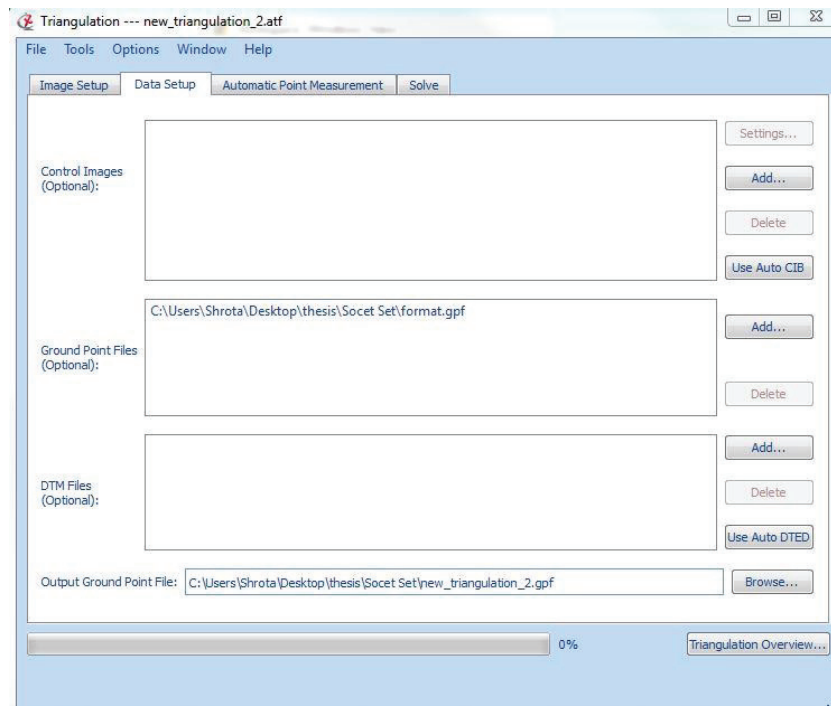


Figure 3-5: Triangulation window with ground point file and APM tab

The solve tab used the method bundle adjustment that minimizes the relative difference between the points measured on overlapping images. The image RMS with pixel value less than 1 is good. The image residual with maximum value were deleted or re-measured. After suitable adjustment, the results were saved.

3.2.3 Automatic Terrain Generation (ATG)

SOCET GXP consists of both Automatic Terrain Extraction (ATE) and Next Generation Automatic Terrain Extraction (NGATE) applications to generate DTM. The main difference between ATE and NGATE is that NGATE provides more accurate and dense DTM and also has option for DTM and/or DSM. The DTM and DSM were generated from using stereo imagery.

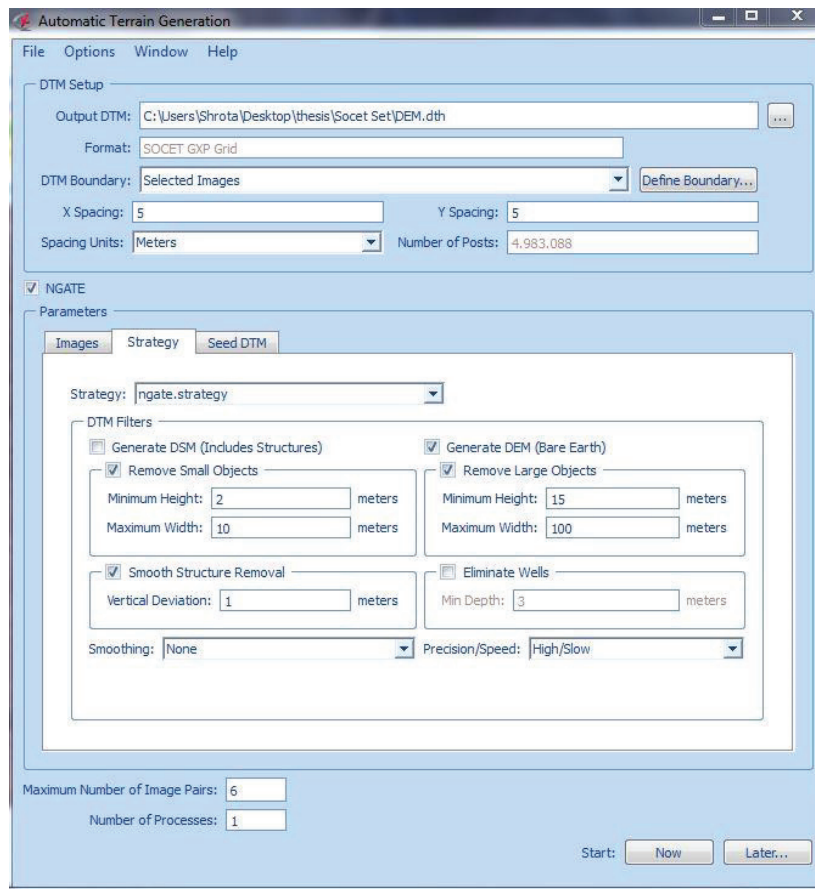


Figure 3-6: Automatic terrain generation tab

The stereo images for the study area were selected with the define boundary on ATG tab. The X and Y spacing for the terrain were selected. NGATE algorithm was selected to generate DTM and DSM.

3.2.4 Extraction of CHM from DSM and DTM

CHM for digital aerial image was extracted by subtracting DTM from DSM using raster calculator on Arc GIS 10.1.

3.3 Regression Analysis

3.3.1 Estimating dominant tree height and basal area from LiDAR data

Eight different predictor variables (i) 25, (ii) 50, (iii) 75 and (iv) 90 percentiles of the height distribution of laser pulses classified as canopy hits, (v) the maximum value, (vi) the mean value, (vii) the coefficient variation, and (viii) canopy density calculated as the number of canopy hits divided by total number of transmitted pulses derived from the laser data were used to develop models to estimate tree height and volume. The canopy height and tree height vary with plots and it is better to model mean height of dominant tree using different quantiles (Naesset and Bjerkness, 2001).

The linear regression that is found to be suitable for estimation of mean height and timber volume look like is

$$l_n h_L = b_0 + b_1 l_n h_{max} + b_2 l_n h_{mean} + b_3 l_n h_{10} + b_4 l_n h_{50} + b_5 l_n h_{75} + b_6 l_n h_{90} + b_7 l_n h_{cv} \quad (1)$$

$$l_n B = b_0 + b_1 l_n h_{max} + b_2 l_n h_{mean} + b_3 l_n h_{10} + b_4 l_n h_{50} + b_5 l_n h_{75} + b_6 l_n h_{90} + b_7 l_n h_{cv} + l_n D_1 \quad (2)$$

Where,

$l_n h_L$ = Lorey's mean height

$h_{10}, h_{50}, h_{75}, h_{90}$ = 10, 50, 75, 90 percentiles of the laser canopy heights

h_{max} = maximum laser canopy height

h_{mean} = mean of the laser canopy height

h_{cv} = coefficient variation of laser canopy heights

B = Basal area (m²/ha)

D_1 = canopy densities corresponding to proportions of laser returns to total number laser returns

3.3.2 Estimating stand volume from LiDAR data

The allometric equation for the stand volume is the multiplicative model of mean LiDAR stand height and mean LiDAR canopy cover density (Naesset, 1997b).

$$V = bhD \quad (3)$$

Where,

V = total volume per hectare with bark (m³/ha)

h = LiDAR stand mean height (m)

D = mean LiDAR canopy cover density

4. Results

4.1 Descriptive analysis of field data

Forest stand parameters (Lorey's height, Basal area, volume) of 24 field plots were considered for analysis of study area. The descriptive statistics of each parameter for the study area are shown in table 4.1. The field plot has *Pinus sylvestris*, *Picea abies*, and *Betula pubescens* species among which *Pinus sylvestris* is the most dominant species.

Table 4-1: Descriptive statistics of field plots

Statistic	Volume(m3/ha)	Basal area(m2/ha)	Lorey's height(m)
Mean	226	259	18
Minimum	55	100	11
Maximum	401	453	24
Std. Deviation	86	78	31

Lorey's mean height, Basal area and Volume of three different species are presented in the box plot as shown in fig 4.1, 4.2 and 4.3. The box plots show that *Pinus sylvestris* has the largest basal area and Lorey's height followed by *Picea abies* and *Betula pubescens* has very low values of Lorey's height and basal area. *Pinus sylvestris* has the largest variation range on basal area and volume followed by *Picea abies*, while least variation on the Lorey's height. Moreover, *Picea abies* has the highest variability on the Lorey's height compare to other species.

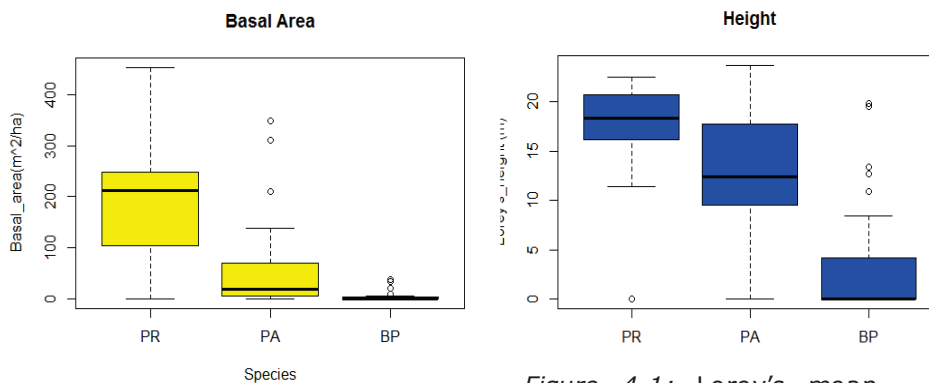


Figure 4-2: basal area PR= Pinus sylvestris, PA= Picea abies, BP= Betula pubescens)

Figure 4-1: Lorey's mean height (PR= Pinus sylvestris, PA= Picea abies, BP= Betula pubescens)

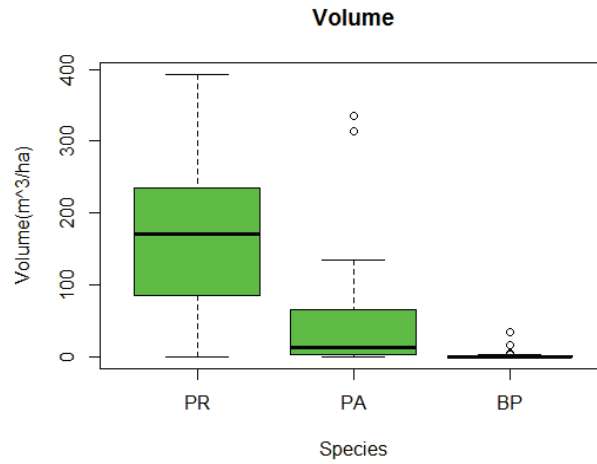


Figure 4-3: volume of major tree species

4.2 DSM, DTM and CHM generation from LiDAR data

The above-ground LiDAR data were filtered to obtain the DTM (Bare earth surface). The Canopy height model (CHM) was then generated using the first returns. The 3D view of the CHM is shown in fig 4.4(b)

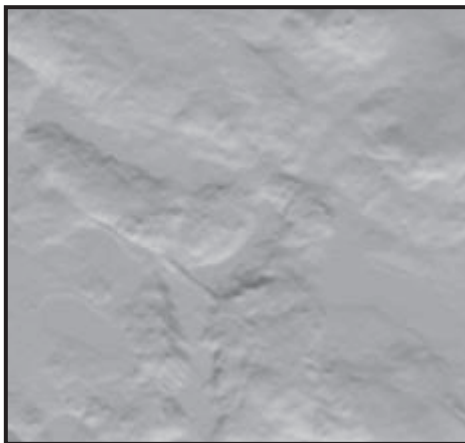
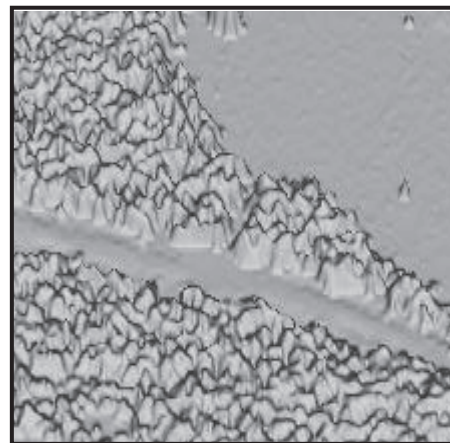


Figure 4-4: (a) DTM and cloud using Fusion software



(b) CHM derived from LiDAR point

4.3 Extraction of field plots from LiDAR data

The circular plot size of radius 8.46 m was masked out from the LiDAR data using XY coordinates. The cross section profile and overhead view is as shown in fig 4.5. Each extracted plot contains LiDAR point clouds used further in calculation of plot metrics. The LiDAR metrics were computed from the 1st returns of LiDAR data.

The canopy cover for this plot on fig 4.5 is 71% whereas the minimum elevation is 240 m, maximum elevation is 264 m. The plot metrics such as maximum, mean, coefficient of variation of LiDAR heights, different quantile- based metrics describing the LiDAR height distribution, canopy density metrics were extracted for each field plots.

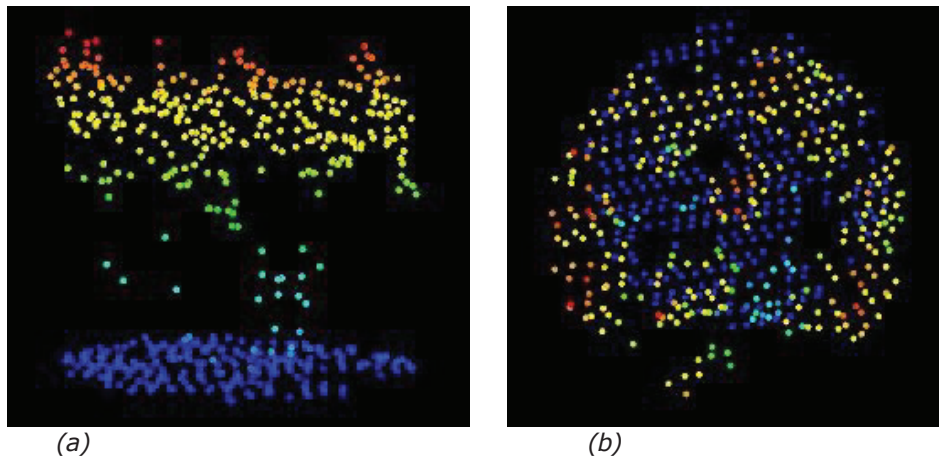


Figure 4-5: Cross-section (a) and overhead view (b) for the same field plot

4.4 Accuracy assessment

4.4.1 LiDAR derived height

Tree height collected from field plots and derived from LiDAR were compared using linear regression model. The comparison was done with 15 field plots. The tree height was computed by relating with seven predictor variables derived from LiDAR. The summary of statistics for both height measurements is given in Table 4.2. On average, field (Lorey's) height overestimated LiDAR derived tree height, by 0.11 m, which is described as tree height of 5 plots were overestimated and remaining 10 plots were underestimated on LiDAR derived height.

Table 4-2: Summary of statistics for tree height measurement

Statistics	Lorey's height(m)	Lidar derived height(m)
Mean	16.97	16.86
Minimum	11	11.78
Maximum	21.2	21.65
Standard deviation	2.97	2.87

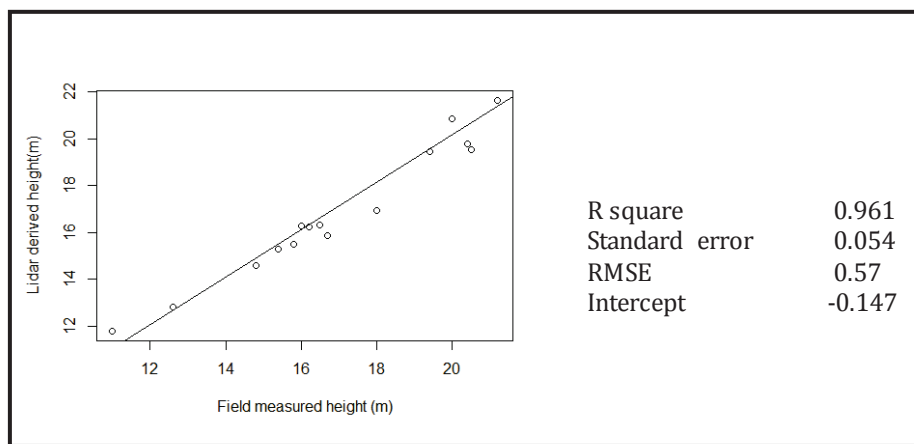


Figure 4-6: Scatterplot and summary of regression for tree height measurements

Goodness of fit between LiDAR derived height and Lorey's height was analyzed on R stat using regression analysis for 15 field plot metrics. R square shows that the LiDAR derived height was predicted at 96% with RMSE of 0.57 m.

The test hypothesis from one way ANOVA at 95% confidence interval and Pearson's correlation test shows that there was significant relationship between Lorey's mean tree height and LiDAR derived mean tree height.

Table 4-3: Summary of ANOVA analysis for tree height

Summary	df	SS	MS	F	Significance F
Regression	1	118.67	118.67	327.81	0.000000132
Residual	13	4.706	0.362		

Total 14 123.373

4.4.2 Basal Area

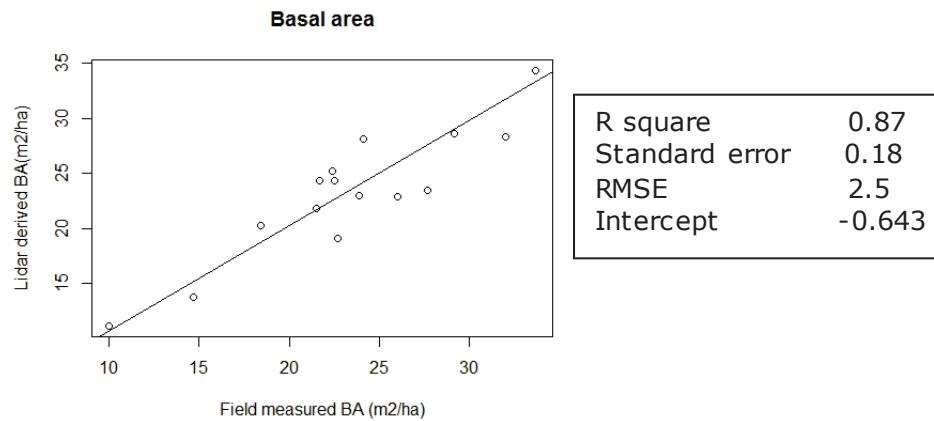


Figure 4-7: Scatterplot and summary of regression for basal area measurements

The basal area was computed within 15 field plots using eight predictor variables derived from LiDAR. The linear regression model for the field measured and LiDAR derived basal area shows that the field measured basal area is 0.10 m²/ha greater than LiDAR derived basal area on average. However, the LiDAR derived basal area underestimate the field measured basal area by 46% and overestimate by 54%.

Table 4-4: Summary of statistics for basal area measurement

Statistics	Field measured BA(m ² /ha)	Lidar derived BA(m ² /ha)
Mean	23.37	23.26
Minimum	10	11.15
Maximum	33.7	34.38
Standard deviation	1.25	1.25

The goodness of fit between basal area from field plot and LiDAR was analysed and regression analysis was done among 15 field plots. The regression shows that LiDAR derived basal area was predicted with 87% and RMSE of 2.5 m. The one way ANOVA at 95% confidence interval and Pearson's correlation test shows that there was significant relationship between field measured basal area and LiDAR derived basal area.

Table 4-5: Summary of ANOVA test for basal area measurement

Summary	df	SS	MS	F	Significance F
Regression	1	433.61	433.61	59.273	3.40E-06
Residual	13	95.1			
Total	14	528.71			

4.5 Correlation analysis

Pearson’s product moment correlation coefficient analysis was performed between LiDAR metrics and Lorey’s mean height. The correlation coefficient for all LiDAR metrics ranges from 0.1 to 0.9. Among the LiDAR metrics, coefficient variations of laser canopy heights (h_{cv}) had the highest correlation coefficient 0.9 and 10th percentiles of laser canopy height (h_{10}) had the least correlation coefficient. The LiDAR metrics have weak relationship with Lorey’s height but have positive correlation.

Table 4-6: Correlation among the variables of regression model

Correlation among LiDAR metrics and Lorey's height					Correlation among LiDAR metrics and BA		
Variables	df(n-2)	t-statistic	r	P value	t-statistic	r	P value
hmax	13	0.6123	0.11	0.55	0.2223	0.06	0.8275
hmean	13	0.3904	0.11	0.70	0.1564	0.04	0.8781
hcv	13	7.898	0.91	0.0000026	2.3953	0.55	0.032
h10	13	0.0764	0.021	0.94	-0.1491	-0.041	0.8838
h50	13	0.653	0.178	0.5252	0.4032	0.11	0.6934
h75	13	0.5982	0.164	0.56	0.23	0.06	0.8217
h90	13	0.6203	0.17	0.55	0.24	0.066	0.8519
D1					-28.786	0.623	0.012

Similarly, correlation coefficient was performed between LiDAR metrics and basal area. The correlation coefficient ranged from -0.21 to 0.44. The correlation coefficient between canopy density and basal

area was the highest while the lowest was with the coefficient variations of LiDAR canopy heights (h_{cv}).

4.6 Stepwise Regression

Stepwise regression procedure was performed to select LiDAR metrics on the final model. The stepwise regression was performed with 7 predictor variables from the LiDAR metrics that was selected to compute the tree height. The least AIC value was selected for the final model. The combination of h_{10} and h_{90} for estimation of the tree height gave the least AIC value. The final model to estimate the tree height is given by means of following equation (4). However, for the basal area model 7 predictor variables were selected among the 8 predictor variables. The multiplicative model for basal area was estimated as linear regression in following form (5):

$$l_n h = b_0 + b_1 l_n h_{10} + b_2 l_n h_{90} \quad (4)$$

Where,

l_n = natural logarithm to the base 2.71828

h = LiDAR derived mean height

b_0 = intercept

b_1 = coefficient of 10th percentiles of LiDAR metrics

b_2 = coefficient of 90th percentiles of LiDAR metrics

$$l_n B = b_0 + b_1 l_n h_{max} + b_2 l_n h_{mean} + b_3 l_n h_{50} + b_4 l_n h_{75} + b_5 l_n h_{90} + b_6 l_n h_{cv} + b_7 l_n D_1 \quad (5)$$

Where,

l_n = natural logarithm to the base 2.71828

B = LiDAR derived basal area

b_0 = intercept

b_1 = coefficient of maximum LiDAR canopy height

b_2 = coefficient of maximum LiDAR canopy height

b_3 = coefficient of 50th percentiles of LiDAR canopy height

b_4 = coefficient of 75th percentiles of LiDAR canopy height

b_5 = coefficient of 90th percentiles of LiDAR canopy height

b_6 = coefficient of coefficient variation of LiDAR canopy height

b_7 = coefficient of canopy cover density

D_1 = canopy cover density

4.7 Model validation of tree height and basal area

The model for height estimation from stepwise regression was validated with nine independent field plots. The Lorey's mean height and LiDAR derived height were plotted as shown in fig 4.4. R^2 value

for the validated height model was found to be 71% with RMSE of 1.3 m. Similarly, the predicted and observed basal area were plotted and R^2 value for the validated model was found to be 78% with RMSE of 4.5 m^2/ha .

The selected regression equation for estimation of tree height (6) and basal area (7) was as follows:

$$l_n h = -5.574 + l_n h_{10} * (-4.722) + l_n h_{90} * 6.248 \quad (6)$$

$$l_n B = 245.445 + l_n h_{P90} * (-7.317) + l_n h_{mean} * 340.074 + l_n D_1 * 24.685 + l_n h_{max} * 215.117 + l_n h_{cv} * 20.859 + l_n h_{50} * 12.271 + l_n h_{75} * (-587.982) \quad (7)$$

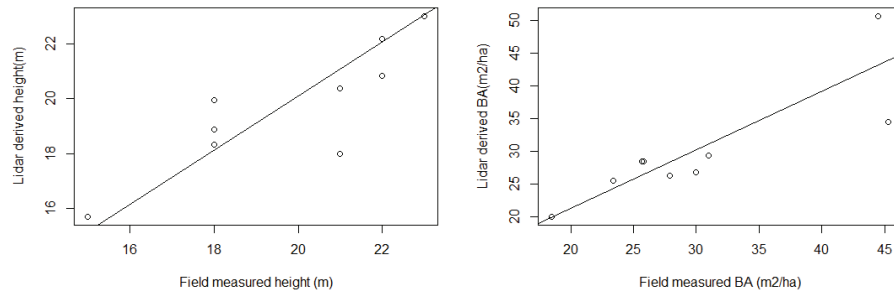


Figure 4-8: Scatterplot of observed and predicted height and basal area

4.8 Model for stand volume

The multiplicative regression model for volume was developed with the combination of canopy density metrics from LiDAR and height derived from eqn. (1). The linear regression for prediction of volume is shown in eqn. (8) with coefficient of height and canopy density.

$$l_n V = b_0 + b_1 l_n h + b_2 l_n D_1 \quad (8)$$

Where,

l_n = natural logarithm to the base 2.71828

V = stand volume

b_0 = intercept

b_1 = coefficient of LiDAR derived height

b_2 = coefficient of canopy density

h = LiDAR derived mean height

D_1 = canopy density

The model was based on the calculation of RMSE and coefficient of determination (R^2). The model has R^2 value of 81% and RMSE of 30.68 m³/ha. The regression coefficients for the model were shown in following table 4.6. The observed and predicted volume from regression models were plotted against each other in fig 4.9. The regression analysis shows that stand volume of 7 field plots were underestimated and remaining 8 field plots were overestimated.

Table 4-7: Regression coefficients and statistics of model

Variables	estiamte	std.error	t value
β_0	-0.6835	0.8589	-0.796
β_1	1.8036	0.,3299	5.467
β_2	-2.3126	1.0143	-2.28
R^2	0.8131		
Adjusted R^2	0.7819		

The test hypothesis from one way ANOVA at 95% confidence interval and Pearson's correlation test shows that there was significant relationship between observed and predicted volume as shown in table 4.7.

Table 4-8: Summary of ANOVA analysis for volume model

Summary	df	SS	M	F	Significance F
Regression	1	56947	56947	52.441	6.54E-06
Residual	13	14114	1086		
Total	14	71061	58033		

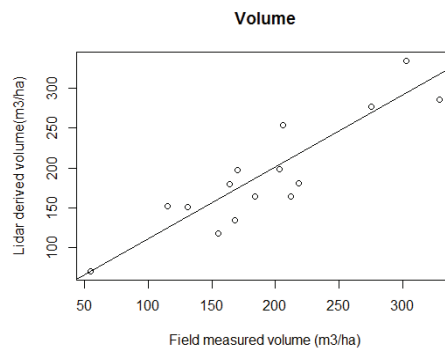


Figure 4-9: Scatterplot of observed and predicted stand volume

4.9 DSM, DTM and CHM generation from aerial 3D image

DSM and DTM from aerial image were generated by using SOCET GXP software to extract CHM. The height difference between DSM and DTM was very low and negative. DSM value for the study area ranged from 60.45 m to 339.46 m while DTM value ranged from 58.53 m to 344.17 m. The value shows that DTM is higher than DSM which cannot be true. The below fig 4.10 shows that DSM and DTM was better to delineate the edges.

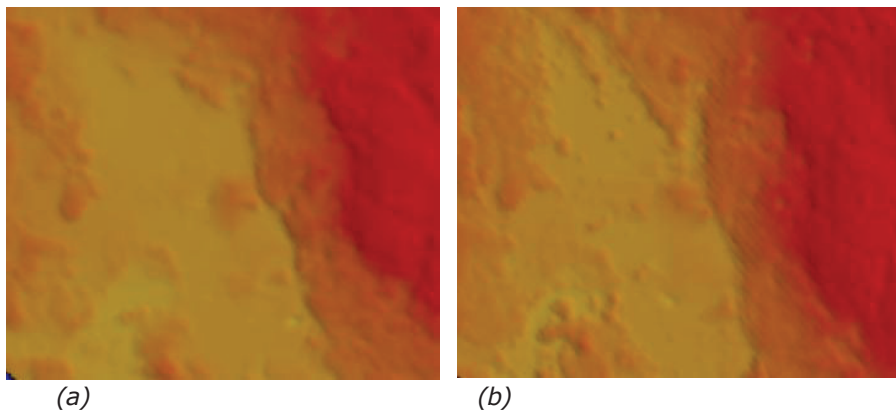


Figure 4-10: shows the (a) DTM and (b) DSM from aerial image

CHM and aerial image of the same area is shown in fig 4.7. The below fig 4-11 shows that aerial image could not generate better CHM over the whole study area. The CHM value for the barren land and forested area were same.

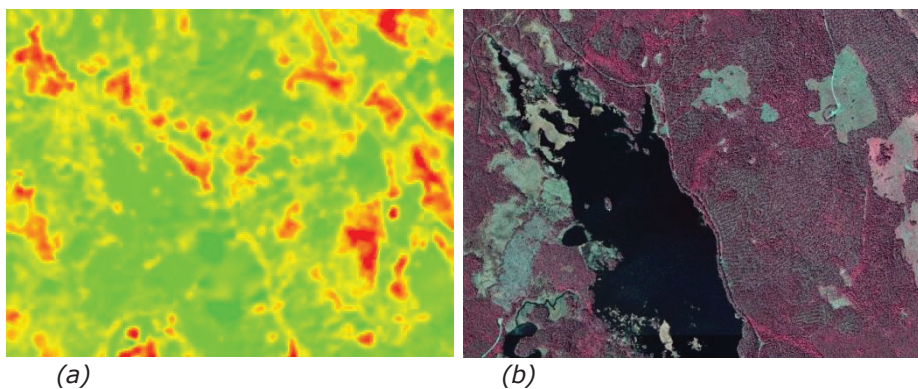


Figure 4-11: shows the (a) CHM and (b) aerial image of the same area

The CHM thus generated from DSM and DTM gave the tree height of 4m on average Whereas, the field measured tree height and LiDAR derived tree height range from 11- 24 m Thus, aerial image was not further processed to estimate the tree height, basal area from the study area. Accurate estimation of CHM requires good quality of DTM and DSM.

5. Discussion

5.1 *Extraction of LiDAR metrics*

48 LiDAR metrics were computed using intensity and elevation values for each field plots. Among these LiDAR metrics, the potential predictor LiDAR metrics had to be selected to estimate the tree height, basal area and volume. The selected LiDAR metrics had to be robust for the estimation of the mean tree height, mean basal area and mean stand volume. Several studies had been done to select the potential LiDAR metrics to estimate the different forest parameters. Næsset and Bjercknes (2001) studies shows that eight predictor variables i.e. (i) 25, (ii) 50, (iii) 75 and (iv) 90 percentiles of the height distribution of laser pulses classified as canopy hits, (v) the maximum value, (vi) the mean value, (vii) the coefficient variation, and (viii) canopy cover density were selected to estimate the dominant height and stem number. Erdody and Moskal (2010), also used nine LiDAR predictor variables which include maximum and mean height, 10th, 25th, 50th, 75th, 90th percentile heights, coefficient of variation of LiDAR heights and canopy density. Similarly, Næsset (2002) used the same eight predictor variables to estimate Lorey's height, dominant height, stem number, basal area and volume. Means (2000) selected 0, 80 and 90 percentiles of the height and 20 percentile of cover to estimate the tree height, basal area and volume. Næsset (1997) studies shows that using mean canopy cover density and LiDAR derived stand mean height can predict the volume of the stand. Therefore, all the LiDAR metrics were not necessary to extract the height, basal area and volume. The potential LiDAR metrics has to be selected according to forest parameters and the predictor variable can be different depending upon the study area, age.

The study area has LiDAR data of 1.0 m point density which is sufficient for estimating tree height, basal area at plot level but not on individual tree level. The LiDAR metrics selected on study area are the potential predictor variables, which estimated the mean tree height and basal area more accurately.

5.2 *LiDAR derived tree height and basal area and accuracy assessment*

The multiple regression analysis was used to develop models to estimate mean tree height, mean basal area using eight predictor variables derived from LiDAR data on 15 field plots.

The LiDAR derived tree height underestimated field measured tree height by 0.11m on average. It showed that 33% of tree height was overestimated and 67% of tree height was underestimated by LiDAR derived tree height compare to Lorey's height. Næsset (1997) research on the mean tree height of forest stands shows that mean laser height underestimated the Lorey's tree height by 4.1-5.5 m. While this study area is young and unmanaged forest, there are some tall trees due to the favourable conditions but there are more small trees and the Lorey's height is also the average of the tree height of sample plot. The study was done in plot level and the value for the tree height is average of plot tree. According to Suárez, Ontiveros et al. (2005), LiDAR underestimate the ground measured tree height by 7-8% with point density of 3-4 points/m². Hyyppä, Hyyppä et al. (2008) study has found that low point density of LiDAR underestimate the tree height. Similarly, the LiDAR point density is 1 point/m² in this study area, thus the percentage difference of overestimation is found low and underestimation is found high.

The coefficient of determination (R^2) of predicted tree height by observed tree height was 96% with RMSE of 0.57m. The Pearson's correlation test and F test shows that there is statistically significant relationship between the Lorey's mean tree height and predicted mean tree height. The finding of this study can be compared with other studies done by several researchers i.e. Næsset (2002) studies obtained R^2 as high as 95% on young forest and this study area is also young forest. Similarly, Andersen, McGaughey et al. (2005) obtained 98% of R^2 with 1.3 m of RMSE, while estimating the canopy height in the coniferous forest. Erdody and Moskal (2010) found 93% of coefficient of determination from LiDAR derived tree height. The different studies shows that coefficient of determination is higher in young forest, it may be due to Lorey's mean height is based on all measured trees while in mature forest it is based on trees with dbh greater than 10cm.

Similarly, the LiDAR derived basal area underestimate the field measured basal area by 46% and overestimate by 54%. The regression shows that LiDAR derived basal area was predicted with 87% and RMSE of 2.5 m. The F test revealed that there is significant relationship between the LiDAR derived basal area and field measured basal area. Næsset, Bollandsås et al. (2005) study revealed that the coefficient of determination is higher in basal area of young forest, which is 91%. Magnussen, Næsset et al. (2011) found 84% of R^2 for LiDAR derived basal area on their study.

The comparison of accuracy of the tree height and basal area cannot be done directly, as there are many factors which influence the accuracy i.e. species, age, crown shape, forest composition, tree density, topographic features and the quality of LiDAR data.

5.3 Model validation of tree height and basal area

Stepwise selection was performed to select LiDAR variables to include in final model and cross validation was done to assess the accuracy. Cross-validation procedure was used to assess the reliability of this model. The cross validation of the model was done with nine independent field plots. R^2 value for the validated mean tree height model was found to be 71% with RMSE of 1.3 m. Similarly, R^2 value for the validated basal area model was found to be 78% with RMSE of 4.5 m²/ha.

Næsset and Bjerknes (2001) study revealed that the after stepwise selection procedure, the final model for tree height include only maximum laser height and coefficient of determination was 75%. Næsset and Gobakken (2005) studies on young forest-stratum comprised of 10th percentiles and mean LiDAR height on the tree height model with 91% R^2 and 0.08 RMSE. While final model of basal area comprised of 10th and 50th percentiles and canopy density with R^2 of 91% and 0.11 RMSE. Monnet (2010) study comprised of 50th, 75th and minimum height values of LiDAR pulses on the final tree height model with 84.1% of R^2 and for final basal area model 25th, 50th percentiles and density metrics was used with R^2 of 70.8%. 10th and 80th percentiles of LiDAR canopy height were selected for prediction of mean tree height on final model while 50th percentiles and mean of LiDAR canopy height and canopy density were selected for final model of mean basal area. Similarly, in this study area, only 10th and 90th percentiles of LiDAR canopy height was included on final tree height model and 7 predictor variables i.e. maximum and mean of LiDAR canopy heights, 50th, 75th and 90th percentiles of LiDAR canopy heights, coefficient of variation of LiDAR canopy heights and canopy cover density was included for the final basal area model.

5.4 LiDAR derived stand volume and accuracy assessment

The mean tree height obtained from final model and LiDAR canopy density metrics were used to estimate the stand volume of the study area. Nelson, Krabill et al. (1988) tested different equations to

compute the best stand volume by using LiDAR canopy density metrics and LiDAR height metrics.

The model of stand volume for this study has R^2 value of 81% and RMSE of 30.68 m³/ha. Næsset, Bollandsås et al. (2005) study has 94% of R^2 on their young forest study area. Linderg, Holmgren et al. (2010) also found 35 m³/ha RMSE on their plot level study area

González-Ferreiro, Diéguez-Aranda et al. (2012) study revealed that the pulses densities of LiDAR affect the quality of DTM and DSM, which in long run will affect the estimation of tree volume and other forest parameters. The comparison between 8 and 0.5 pulses m⁻² in that study shows that R^2 of 8 pulses m⁻² has 10.4% higher than 0.5 pulses m⁻². RMSE of stand volume is larger which is due to smaller mean stem volume, as forest is young. . The total plot volume on field was computed as the sum of individual tree volumes of dbh greater than 4cm on young forest. However, LiDAR cannot easily penetrate the tree canopy and estimate more volume of stand.

Næsset (1997) compared different model to estimate the stand volume and found R^2 range from 46-89% and RMSE of 26-83 m³/ha. This fact also reveals that volume model should be calibrated individually for different tree species. The common volume equation for different species such as Norway spruce, Scots pine tend to underestimate the volume of pure pine stands (Næsset 1997). In this study, the common volume equation was proposed for both Norway spruce and Scots pine. Thus, the RMSE is higher in study area compare to other studies.

5.5 Aerial image analysis

The DSM and DTM generated from LiDAR gave far better result than the aerial image, which in long run affect the quality of CHM. The mean tree height and mean basal area was difficult to estimate from the DSM and DTM generated from aerial image. Thus, the comparison of mean tree height, mean basal area and stand volume from aerial image with LiDAR has to be terminated. Baltsavias (1999) found that LiDAR had strengths on mapping of surface whereas image matching from aerial image delivered poor result. Eid, Gobakken et al. (2004) revealed that LiDAR gave more precise estimates of height, basal area and number of trees than compare to aerial image. Holopainen (2008) studies showed that LiDAR performed far better than aerial photograph while adding aerial photographs features into LiDAR features gave worst result. Hopkinson, Hayashi et al. (2009) compared DEM from LiDAR and aerial photo in their study and found

that LiDAR DEM performed far better than aerial photo DEM. However, aerial photo DEM was able to capture break line features such as ridges and cliff edges. The below figure from the study area also shows that aerial image is able to capture the edges and better for demarcation.

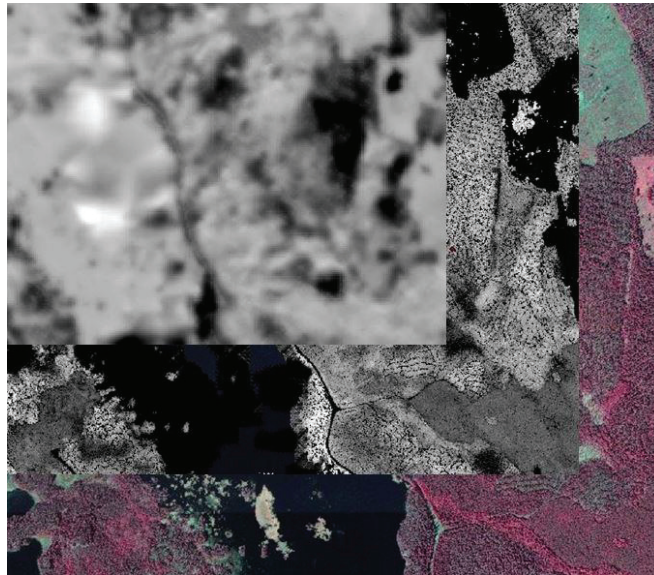


Fig 5- 1 Comparison of CHM derived from aerial image, LiDAR and aerial photographs of the same area from up to bottom respectively

In this study, the aerial image GSD was 0.5 m and not enough overlap aerial image was the major problem to get the poor DSM and DTM. Schardt (2004) suggested that while using photogrammetric methods for forestry purposes, it is better to use DEM from LiDAR to get accurate estimation. The study also found that aerial photographs were not suitable to measure the individual tree heights. Waser (2006) used 0.5 m aerial image to predict the shrub occurrence. Baltsavias, Gruen et al. (2008) used aerial image of GSD 9-22 cm and 60-80% forward overlap to generate high quality DSM and suggested that the accuracy of DSM depends upon the image scale, image texture, imaging geometry and compactness of tree canopy definition. In this study area, digital aerial image has 60% forward overlap and 20-30% side overlap. Due to low GSD and low forward overlap of aerial image could not generate better CHM. The more forward overlap on aerial image will help to generate more tie points on aerial triangulation and which will generate more accurate DTM and DSM.

6 Conclusion and Recommendations

6.1 Conclusions

The objective of this study was to compare the accuracies of estimation of forest parameters using digital aerial image and LiDAR data and to extract the potential LiDAR metrics to generate more accurate height, basal area and volume.

The potential LiDAR metrics that generate accurate tree height and basal area were selected from stepwise procedure and validate with field plots. The 10th and 90th percentiles LiDAR canopy height was selected among seven predictor LiDAR metrics to validate the tree height model and gave 71% of R². Whereas, seven predictor LiDAR metrics were selected among eight LiDAR metrics to validate basal area model and has 78% of R². The model for stand volume comprise of mean tree height generated from final tree height model and canopy cover density generated from LiDAR. In this study, the volume generated from LiDAR has strong relationship with field measured stand volume.

The LiDAR gave the better result compare to aerial image. The aerial image did not generate the better DSM and DTM, which gave poor quality CHM. Thus, the tree height cannot be generated and has to terminate the process of extracting height, basal area and volume.

6.2 Recommendations

The use of digital aerial image has high scope on estimation of forest parameters but should be used with high GSD and high forward overlap digital aerial image. There were some difficulties with digital aerial image during the research time. However, some recommendations are as follows:

- The GSD of aerial image should be at least 25cm to generate accurate CHM from DSM and DTM of aerial images.
- The forward overlap of aerial image should be 75% to generate accurate CHM.
- The knowledge of potential software to generate DSM and DTM from aerial image is necessary requirements to the researcher.
-

References

- Andersen, H.-E., R. J. McGaughey, et al. (2005). "Estimating forest canopy fuel parameters using LIDAR data." Remote Sensing of Environment **94**(4): 441-449.
- Balenovic, I. S., A. Pernar, R. Marjanovic, H. Vuletic, D. Paladinic, E. Kolic, J. Benko, M. (2012). "Digital Photogrammetry - State of the art and potential for application in forest management in Croatia." SEEFOR(South- East European Forestry) **2**(2): 81-93.
- Baltsavias, E., A. Gruen, et al. (2008). "High-quality image matching and automated generation of 3D tree models." International Journal of Remote Sensing **29**(5): 1243-1259.
- Baltsavias, E. P. (1999). "A comparison between photogrammetry and laser scanning." ISPRS Journal of photogrammetry and remote sensing **54**: 83-94.
- Bohlin, J., J. Wallerman, et al. (2012). "Forest variable estimation using photogrammetric matching of digital aerial images in combination with a high-resolution DEM." Scandinavian Journal of Forest Research **27**(7): 692-699.
- Cramer, M. (2005). Digital airborne cameras-status and future.
- Cramer, M., Haala, N. (2009). DGPF Project: Evaluation of digital photogrammetric aerial based imaging systems- overview and results from the pilot centre. Photogrammetry week 2009, University of Stuttgart, Institute for photogrammetry.
- Dandois, J. P. and E. C. Ellis (2010). "Remote Sensing of Vegetation Structure Using Computer Vision." Remote Sensing **2**(4): 1157-1176.
- Eid, T., T. Gobakken, et al. (2004). "Comparing stand inventories for large areas based on photo-interpretation and laser scanning by means of cost-plus-loss analyses." Scandinavian Journal of Forest Research **19**(6): 512-523.
- Erdody, T. L. and L. M. Moskal (2010). "Fusion of LiDAR and imagery for estimating forest canopy fuels." Remote Sensing of Environment **114**(4): 725-737.

- Gong, P., G. S. Biging, et al. (1999). "Photo Ecometrics for Forest Inventory." Geographic Information Sciences **5**(1): 9-14.
- Gong, P., Sheng, Y., and Biging, G.S., (2002). 3d Model- based tree measurement from high resolution aerial imagery, American society for Photogrammetry and Remote sensing
- González-Ferreiro, E., U. Diéguez-Aranda, et al. (2012). "Estimation of stand variables in Pinus radiata D. Don plantations using different LiDAR pulse densities." Forestry **85**(2): 281-292.
- Gulch, E. (2009). Advanced matching techniques for high precision surface and terrain models. Photogrammetry week 2009, University of Stuttgart, Institute for photogrammetry.
- Haala, N. (2009). Come back of digital image matching. Photogrammetric week 2009, University of Stuttgart, Institute for photogrammetry.
- Holopainen, M., Talvitie, M., (2004). Forest inventory by means of tree wise 3D measurements of laser scanning data and digital aerial photographs. Remote sensing and Spatial information sciences, International archives of photogrammetry.
- Holopainen, M. H., R. Tuominen, S. Viitala, R. (2008). Performance of airborne laser scanning and aerial photograph based statistical and textural features in forest variable estimation. SilviLaser, Edinburg, UK.
- Hopkinson, C., M. Hayashi, et al. (2009). "Comparing alpine watershed attributes from LiDAR, Photogrammetric, and Contour-based Digital Elevation Models." Hydrological Processes **23**(3): 451-463.
- Hyypä, J., H. Hyypä, et al. (2008). "Review of methods of small-footprint airborne laser scanning for extracting forest inventory data in boreal forests." International Journal of Remote Sensing **29**(5): 1339-1366.
- Junttila, V. (2011). Automated, Adaptive methods for forest inventory. Lappeenranta, Finland, Lappeenranta University of Technology: 65.

Kamiya, T. K., H. Wang, J. Itaya, A. (2012). Forest resource management system by standing tree volume estimation using aerial stereo photos. XXII ISPRS congress, Melbourne , Australia.

Kangas, A., E. Heikkinen, et al. (2004). "Accuracy of partially visually assessed stand characteristics: a case study of Finnish forest inventory by compartments." Canadian Journal of Forest Research **34**(4): 916-930.

Ke, Y., Quackenbush, J.L. (2009). Individual tree crown detection and delineation from high spatial resolution imagery using active contour and hill climbing methods. ASPRS Annual conference, Baltimore, Maryland.

Korpela, I. (2004). Individual tree measurements by means of digital aerial photogrammetry, Finnish Society of Forest Science.

Kukko, A., and Hyypä (2009). "Small foot print laser scanning simulator for system validation, error assessment, and algorithm development." Photogrammetric Engineering and Remote sensing **75**(9): 1177- 1189.

Leberl, F. I., A. Pock, T. Meixner, P. Gruber, M. Scholz, S. & Wiechert, A. (2010). "Point clouds: Lidar versus 3D vision." Photogrammetry Engineering & Remote Sensing **76**(10): 1123-1134.

Lemaire, C. (2008). Aspects of the DSM production with high resolution images. Remote sensing and spatial information sciences, Beijing, China, The International archives of the photogrammetry

Lillesand T. M. & Kiefer R. W. (2000). Remote Sensing and Image Interpretation, Wiley & Sons.

Linderg, E., J. Holmgren, et al. (2010). "Estimation of tree lists from airborne laser scanning by combining single-tree and area-based methods." International Journal of Remote Sensing **31**(5): 1175-1192.

Lothammer, K. H. (2008). Aspects of DSM production. Proceedings of Map Asia 2008, Kuala Lumpur, Malaysia.

Madani, M. (2001). Importance of Digital Photogrammetry for a complete GIS. 5th Global Spatial Data Infrastructure Conference, Cartagena, Columbia.

Magnussen, S. and P. Boudewyn (1998). "Derivations of stand heights from airborne laser scanner data with canopy-based quantile estimators." Canadian Journal of Forest Research **28**(7): 1016-1031.

Magnussen, S., E. Næsset, et al. (2011). "A fine-scale model for area-based predictions of tree-size-related attributes derived from LiDAR canopy heights." Scandinavian Journal of Forest Research **27**(3): 312-322.

Magnusson, M. (2006). Evaluation of Remote sensing techniques for estimation of forest variables at stand level. Department of Forest Resource Management and Geomatics. Umeå, Sweden, Swedish University of Agricultural Sciences. **Doctoral thesis**.

Magnusson, M., J. E. S. Fransson, et al. (2007). "Aerial photo-interpretation using Z/I DMC images for estimation of forest variables." Scandinavian Journal of Forest Research **22**(3): 254-266.

McGaughey, R. J., Andersen, H. E., & Reutebuch, S.E. (2006). Considerations for planning, acquiring, and processing LIDAR data for forestry applications. In Proceedings of the eleventh Biennial USDA Forest Service Remote Sensing Applications Conference, Salt Lake City, American Society of Photogrammetry and Remote Sensing.

Means, J. E. A., S. A. Fitt, B.J. Renslow, M. Emerson, L. and Hendrix, C. J. (2000). Predicting Forest Stand Characteristics with Airborne Scanning Lidar. Photogrammetric Engineering & Remote Sensing 2000 American Society for Phtogrammetry and Remote Sensing.

Monnet, J. M. M., E. Chanussot, J. Berger, F. (2010). Estimation of forest parameters in mountainous coppice stands using airborne laser scanning. Silvilaser 2010. Freiburg, Germany, 10th International Conference in LiDAR applications for forest assessing forest ecosystems. **1-4**.

Næsset, E. (1997). "Estimating timber volume of forest stands using airborne laser scanner data." Remote Sensing of Environment **61**(2): 246-253.

Næsset, E. (2002). "Predicting forest stand characteristics with airborne scanning laser using a practical two-stage procedure and field data." Remote Sensing of Environment **80**(1): 88-99.

Næsset, E. and K.-O. Bjerknes (2001). "Estimating tree heights and number of stems in young forest stands using airborne laser scanner data." Remote Sensing of Environment **78**(3): 328-340.

Næsset, E., O. M. Bollandsås, et al. (2005). "Comparing regression methods in estimation of biophysical properties of forest stands from two different inventories using laser scanner data." Remote Sensing of Environment **94**(4): 541-553.

Næsset, E. and T. Gobakken (2005). "Estimating forest growth using canopy metrics derived from airborne laser scanner data." Remote Sensing of Environment **96**(3-4): 453-465.

Nelson, R., W. Krabill, et al. (1988). "Estimating forest biomass and volume using airborne laser data." Remote Sensing of Environment **24**(2): 247-267.

Olsson, H., Egberth, M., Engberg, J., Franssion, J.E.S., pahlen, T.G., Hagner, O., Holmgren, J., Joyce, S., Magnusson, M., Nilsson, B., Nilsson, M., Olofsson, K., Reese, H., Wallerman, J. (2005). Current and emerging operational uses of remote sensing in swedish forestry. Proceedings of the seventh annual forest inventory and analysis symposium, US forest service, Portland, USA.

Packalen, P. (2009). Using Airborne laser scanning data and digital aerial photographs to estimate growing stock by tree species. Faculty of forest sciences. Finland, University of Joensuu.

Potuckova, M. (2004). Image matching and its applications in photogrammetry. Faculty of Civil engineering. Denmark, Czech Technical University, prague.

Schardt, M. H., W. Hirschmugl, M. Wack, R. Franke, M. (2004). Comparison of aerial photographs and laser scanning as methods for obtaining 3D forest stand parameters. International archives of photogrammetry, remote sensing and spatial information sciences.

Sohraib, H. (2012). Estimating mixed broad leaved forest stand volume using DSM extracted from digital aerial images. International archives of the photogrammetry, Melbourne, Australia, Remote sensing and spatial information sciences.

Suárez, J. C., C. Ontiveros, et al. (2005). "Use of airborne LiDAR and aerial photography in the estimation of individual tree heights in forestry." Computers & Geosciences **31**(2): 253-262.

Tomppo, E., Gschwantner, T., Lawrence, M., McRoberts, R.E, Ed. (2010). National Forest Inventories, pathway for common reporting. XXVI, Springer books.

Tuominen, S. and A. Pekkarinen (2005). "Performance of different spectral and textural aerial photograph features in multi-source forest inventory." Remote Sensing of Environment **94**(2): 256-268.

Waser, L. T., E. Baltsavias, et al. (2008). "Assessing changes of forest area and shrub encroachment in a mire ecosystem using digital surface models and CIR aerial images." Remote Sensing of Environment **112**(5): 1956-1968.

Waser, L. T., Ecker, K. Ginzler, C. Kuchler, M. Schwarz, M. & Thee, P. (2006). Extraction of forest parameters in a mire environment using airborne spectral data and digital surface models. Workshop on 3D remote sensing in forestry, Vienna.

Wulder, M. A., Franklin, S.E., Ed. (2003). Remote sensing of Forest Environments. Concepts and case studies. USA, Kluwer Academic Publisher.

Yuan, X. (2008). "On stereo model reconstitution in aerial photogrammetry." Geo-spatial Information Science **11**(4): 235-242.

Zagalikis, G., A. D. Cameron, et al. (2005). "The application of digital photogrammetry and image analysis techniques to derive tree and stand characteristics." Canadian Journal of Forest Research **35**(5): 1224-1237.

Zhang, B., Miller, S., DeVencia, K., Walker, S., (2006). Automatic terrain extraction using multiple image pair and bacI matching. ASPRS 2006 Annual conference, Reno, Nevada.